

Effect of disorder on the temperature dependence of the resistivity of SrRuO₃

G. Herranz,^{1,*} V. Laukhin,² F. Sánchez,¹ P. Levy,³ C. Ferrater,⁴ M. V. García-Cuenca,⁴ M. Varela,⁴ and J. Fontcuberta¹

¹*Institut de Ciència de Materials de Barcelona (ICMAB-CSIC), Campus UAB, Bellaterra 08193, Catalunya, Spain*

²*Institució Catalana de Recerca i Estudis Avançats (ICREA), Barcelona 08010, Spain,*

and ICMAB-CSIC Campus UAB, Catalunya, Bellaterra 08193, Spain

³*Departamento de Física, CAC, CNEA, Avenida Gral Paz 1499 (1650), San Martín, Buenos Aires 1650, Argentina*

⁴*Departament de Física Aplicada i Òptica, and Institut de Nanociència i Nanotecnologia (IN2UB),*

Universitat de Barcelona, Diagonal 647, Catalunya, Barcelona 08028, Spain

(Received 26 July 2007; revised manuscript received 7 October 2007; published 10 April 2008)

We have investigated the effect of structural disorder on the temperature dependence of the resistivity $\rho(T)$ of epitaxial SrRuO₃ films. Distinctive effects of disorder are seen at low and high temperatures. For temperatures well below the ferromagnetic transition and above the region where quantum effects set in, the observed nonlinear $\rho(T)$ can be interpreted within a two-fluid electronic model in which a fraction of electronic states are delocalized and the remaining fraction correspond to carriers trapped in localized states induced by disorder. On the other hand, at temperatures above the ferromagnetic transition, the temperature dependence is linear, but remarkably it is found that the slope of $\rho(T)$ *increases* as disorder increases. This latter result is radically dissimilar to what is observed in other complex electronic systems, where disorder commonly induces a reduction of the slope.

DOI: 10.1103/PhysRevB.77.165114

PACS number(s): 72.10.Di, 72.15.Rn, 73.50.Bk

SrRuO₃ is a ferromagnetic oxide ($T_C \approx 150$ K) with metallic behavior. Due to their good conductivity, SrRuO₃ thin films are used as electrodes in oxide heterostructures.¹ For that reason, several studies have focused on the temperature dependence of the electrical resistivity $\rho(T)$ of SrRuO₃ thin films. In this regard, both low-temperature (well below T_C) and high-temperature (above T_C) $\rho(T)$ curves have been analyzed. Considering the low- T regime, it has been found that SrRuO₃ films with low residual resistivity ($\rho < 8 \mu\Omega \text{ cm}$) show a T^2 dependence at $T \leq 10$ K,² but at $10 \text{ K} < T < T_C$, a puzzling sample-dependent temperature power law given by $\rho(T) = \rho_0 + AT^n$, with n varying between 1 and 2, has been reported.³ Concerning the high- T regime, a nearly linear temperature dependence of the resistivity is observed up to temperatures as high as 1000 K.³ This is in clear contrast with other strongly correlated systems, such as the A15 compounds, where a “resistivity saturation” effect is observed at high temperature.^{4,5} It has been proposed that this phenomenon is intimately related to disorder.^{5,6} However, quite remarkably, there has not been any systematic study of the effect of disorder on the linear T dependence of the resistivity of SrRuO₃ films, where the resistivity saturation effect is not observed.³ We should also emphasize that SrRuO₃ stands for a good model for the analysis of the effects of disorder in the electronic transport of strongly correlated systems, contrary to other complex systems such as manganites, where electronic phase segregation^{7,8} eventually driven by disorder⁹ may mask the intrinsic effects.

In this paper, we take advantage of our ability to control the specific degree of structural disorder in SrRuO₃ films via growth mechanisms or ion irradiation to analyze the sensitivity of the resistivity to disorder both at the low- and the high-temperature regimes. We show that the low- T dependence of resistivity follows a power law with exponent n , which varies in a systematic way with disorder. To explain this correlation, we propose a two-fluid electronic model with a disorder-dependent ratio of localized and/or delocal-

ized electronic states, with temperature-dependent relative occupation numbers. On the other hand, we show that for moderate amount of disorder, the slope of the linear $\rho(T)$ dependence of the high- T regime *increases* with disorder. Although a similar phenomenon has been observed, e.g., for the Ce_{3-x}S₄ series (see Fig. 1 in Ref. 10), this observation is in contrast to what is observed in A15 compounds, where disorder induces a reduction of the slope.^{4,11}

SrRuO₃ films have been grown by pulsed laser deposition on SrTiO₃ (001) substrates with a KrF ($\lambda = 248$ nm) excimer laser. The films are fully epitaxial. We have performed extensive structural and morphological characterization of our samples, including high resolution x-ray diffraction,¹² μ -Raman spectroscopy,¹² and extensive atomic force microscopy analysis.^{13,14} We have used two different protocols to modulate accurately the amount of structural disorder in the films. In previous reports, we have demonstrated that the structural disorder depends on the details of the early stage of film growth, which, in turn, depend on the substrate vicinity.¹² Bearing this in mind, films of series Ai ($i = 1-4$) with nanometric thickness (3.5 and 7 nm) were grown on SrTiO₃ substrates with different miscut angles ($0^\circ \leq \theta \leq 2^\circ$). As an additional way to modulate the structural disorder, in series Bi ($i = 1-3$), films with thickness $t = 20$ nm have been irradiated with different doses of accelerated Ar⁺ ions with the same kinetic energy (100 keV). A list of all the samples analyzed here is displayed in Table I. The electrical resistivity of the samples has been measured by using the conventional four-probe method.

In Fig. 1, we show the $\rho(T)$ curves measured for all films. We focus first on the low-temperature region below the Curie temperature. At the lowest temperatures, resistivity upturns at temperatures $2 \text{ K} \leq T_{\min} \leq 30 \text{ K}$ are observed. A source for these upturns might be a Kondo resonance originated by the exchange interaction between magnetic impurities and delocalized carriers, as occurs in diluted magnetic metallic alloys.¹⁵ This is not, however, the case in our SrRuO₃ thin

TABLE I. List of samples analyzed in this paper.

Samples	T_{\min} (K)	γ ($\mu\Omega$ cm K^{-1})	n	A_{ph} ($\mu\Omega$ cm K^{-1})	E_g (K)
A1 (7 nm, 2°)	6.3	0.58	1.3	1.29	25.4
A2 (3.5 nm, 2°)	10.1	0.74	1.4	1.9	28.6
A3 (3.5 nm, 0°)	19.7	1.11	1.9	3.69	31.6
A4 (3.5 nm, 1.5°)	31.4	1.36	2.4	5.52	37.7
B1 (10^{12} cm $^{-2}$)	2.0	0.78	1.15	1.98	21.2
B2 (5×10^{12} cm $^{-2}$)	4.0	0.83	1.4	2.06	25.9
B3 (10^{13} cm $^{-2}$)	9.0	1.09	1.7	2.31	30.9

films. Indeed, we have previously shown that these resistivity upturns are originated by disorder-enhanced quantum interference of carrier wave functions.^{16,17} Confirming our previous results,¹⁶ we have verified that there is a direct correlation between T_{\min} and the residual resistivity for the samples analyzed here, indicating that T_{\min} is a precise parameter to quantify the effects of the structural disorder. To avoid any influence from the quantum effects, we have restricted the analysis of $\rho(T)$ to temperatures well above T_{\min} . We present here the results from the analysis at a temperature range of $40 \text{ K} \leq T \leq 80 \text{ K}$. We should stress, however, that we have checked that extending the analysis to other intervals in the 30–100 K temperature range does not modify the conclusions shown below. We present also the results of the analysis in the temperature range of $170 \text{ K} \leq T \leq 300 \text{ K}$. Note that the analyzed ranges are not close to the Curie temperature ($T_C \approx 150 \text{ K}$) and, thus, the effect of spin-spin fluctuations in the transport is minimized.

Low-temperature region ($T < T_C$). Following the common wisdom,³ we have initially assumed that the resistivity can be described by a power law,

$$\rho(T) = \rho_0 + AT^n. \quad (1)$$

In order to find out the correct exponent n , we have proceeded to a least-squares minimization of fittings of the ex-

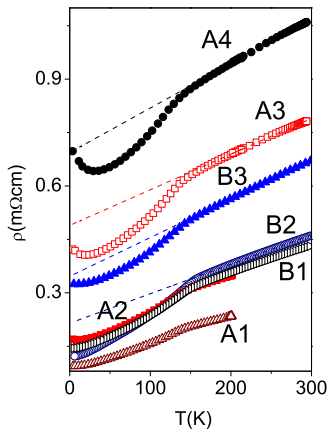


FIG. 1. (Color online) (a) Temperature dependence of the resistivity of SrRuO₃ films. The samples are labeled according to Table I. The dotted lines are the fittings to the high- T linear regime.

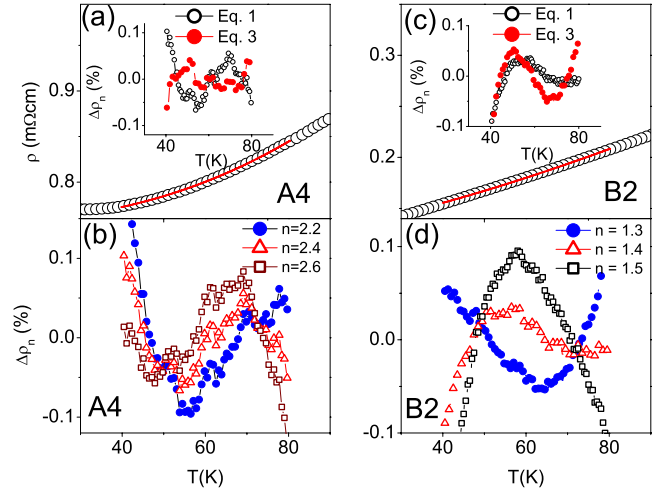


FIG. 2. (Color online) In panels (a) and (c), the open symbols correspond to the temperature dependence of the resistivity $\rho(T)$ of samples A4 and B2, respectively (see Table I). The solid lines are the fittings of $\rho(T)$ to Eq. (1). Insets: the deviation plots, defined as $\Delta\rho_n = [\rho_{fitting}(T) - \rho(T)]/\rho(T)$, are plotted for the fittings to Eqs. (1) and (3) of data for samples (a) A4 and (c) B2. In panels (b) and (d), $\Delta\rho_n$ is shown for different values of the power-law index n for $\rho(T)$ data of samples (b) A4 and (d) B2 fitted to Eq. (1).

perimental resistivity data to Eq. (1) by varying n . The same fittings yielded also the corresponding factor A . Solid lines through the experimental data in Figs. 2(a) and 2(c) show representative fittings of $\rho(T)$ to Eq. (1) corresponding to samples A4 and B2, respectively. As a means to evaluate the quality of these fittings, we have calculated the deviation plots, defined as $\Delta\rho_n = [\rho_{fitting}(T) - \rho(T)]/\rho(T)$, as a function of the temperature for fittings made varying the exponent n . In Figs. 2(b) and 2(d), we show the deviation plots obtained for different n values for samples A4 and B2. We clearly see that $\Delta\rho_n$ is minimized for optimized values of n . Thus, deviation plots allow accurate determination of n and A for each sample.

In Fig. 3, we plot the values of T_{\min} vs the corresponding n extracted from fittings to Eq. (1) for all films of series A and series B vs the corresponding T_{\min} . Data in this figure

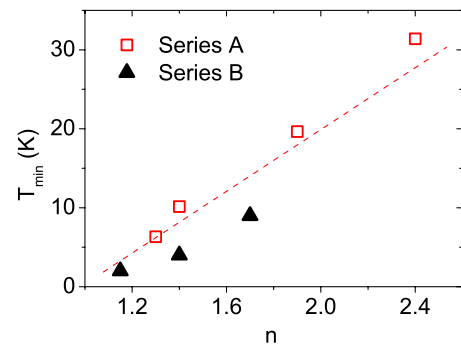


FIG. 3. (Color online) Correlation between the resistivity upturn temperature T_{\min} and the fractional power-law index n [Eq. (1)] for SrRuO₃ films of series A (open squares) and series B (closed triangles). The dashed line is a guide for the eyes.

unequivocally show that n increases with disorder, ranging from $n \approx 1.1$ for weak disorder to $n \approx 2.4$ for stronger disorder. From this analysis, we conclude that temperature dependence of the resistivity is progressively more nonlinear as disorder increases. Reversely, we also find that $n \rightarrow 1$ as disorder is reduced, suggesting that linear temperature dependence in the interval $40 \text{ K} \leq T \leq 80 \text{ K}$ is approached in the weakest disorder limit. We investigated a possible magnetic contribution to the observed power law by fitting to Eq. (1) the $\rho(T)$ data measured in a strong field $H=48 \text{ T}$ (see Ref. 17). We have verified that the power-law exponent n is not affected by such strong fields and, thus, we can exclude any relevant magnetic contribution to the observed low- T resistivity dependence. In the following, we discuss a possible physical mechanism to explain the correlation between n and the disorder.

Recently, Kumar and Majumdar¹⁸ have suggested a microscopic model to explain the strong evolution of the low-temperature transport properties of A15 compounds with disorder, which show some parallels with the properties observed in our SrRuO₃ films.¹⁹ In that case, A15 compounds showed a suppression of the temperature dependence of the resistivity for increasing disorder. The model proposed in Ref. 18 describes the effects of disorder on strongly coupled electron-phonon systems. It can be interpreted within a “two fluid” framework, where there is a strong localization (Anderson localization) of a fraction f of charge carriers, whereas there is still a remaining distribution $(1-f)$ of delocalized states near the Fermi energy. The fraction f increases with increasing disorder and residual resistivity. The conductance values of these parallel conduction channels have a relative weight that changes with temperature. The fraction f decreases with increasing temperature due to the thermal induced detrapping or delocalization of localized states thus increasing conductivity. On the other hand, delocalized electrons are scattered by thermal lattice fluctuations contributing to the phonon-limited $\rho(T)$. The two competing tendencies lead, in agreement with experimental data, to a modulation of the low- T dependence of the resistivity on disorder.

Therefore, it is worthwhile to analyze our data within the framework of a two-fluid model. We assume that at $T=0 \text{ K}$, there is a density n_{l0} of localized electronic states, whereas n_{i0} is the density of delocalized states. At $T>0 \text{ K}$, due to thermal excitations, the effective density of carriers in trapped states is reduced to $n_l(T) = n_{l0}[1 - \exp(-E_g/k_B T)]$, whereas the density of them in delocalized states increases by

$$n_i(T) = n_{i0} + n_{l0} \exp(-E_g/k_B T), \quad (2)$$

where E_g is a disorder-dependent energy gap and k_B is the Boltzmann constant. Its microscopic meaning will be discussed below. We further assume that the conductivity σ_l of carriers trapped in localized states is far smaller than the conductivity σ_i of the itinerant carriers, so that the conductivity of samples is $\sigma \approx \sigma_i$. In that case, the resistivity will be modulated by the contribution of itinerant carriers excited thermally across the gap so that $\rho_i = 1/\sigma_i = m_{eff}/[n_i(T)e^2\tau(T)]$, where m_{eff} is the effective

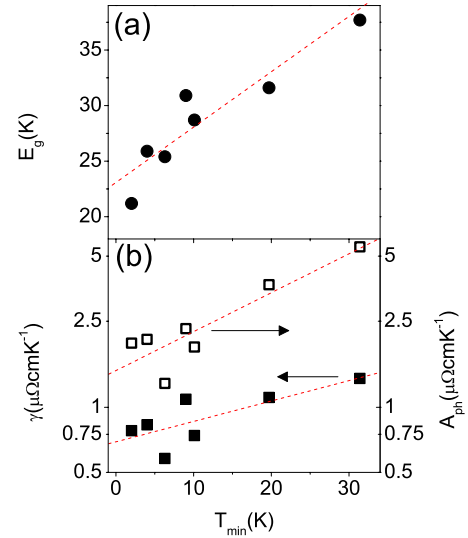


FIG. 4. (Color online) (a) Dependence on disorder (T_{\min}) of the gap E_g extracted from fittings of the low- T $\rho(T)$ of samples A1–A4 and B1–B3 to Eq. (3). (b) Evolution with T_{\min} of coefficients A_{ph} [Eq. (3), open squares] and γ [Eq. (4), closed squares]. Dashed lines are guides for the eyes.

mass and $\tau(T)$ is the scattering time. Taking into account Eq. (2), we find that the low- T resistivity is described by

$$\rho_i(T) = \frac{\rho_0 + A_{ph}T}{1 + n_{l0}/n_{i0} \exp(-E_g/k_B T)}, \quad (3)$$

where it is assumed a linear in T contribution with a linear coefficient A_{ph} coming from the electron-phonon coupling. We have proceeded to fit $\rho(T)$ data for samples from both A and B series in the range of $40 \text{ K} \leq T \leq 80 \text{ K}$ by using Eq. (3). We stress that the scenario represented by Eq. (3) only applies at temperatures above the onset of quantum corrections to transport, and thus it is restricted to $T > T_{\min}$. It turned out that the fitted $\rho(T)$ data using Eq. (3) are virtually indiscernible from results obtained using Eq. (1). Indeed, from the comparison of the deviation plots $\Delta\rho_n$ calculated as described above, it turns out that the quality of fits of resistivity data to Eq. (3) is similar to those fitted to Eq. (1) [see the insets of Figs. 2(a) and 2(c)]. The gap values E_g extracted from fittings to Eq. (3) are plotted in Fig. 4(a) as a function of T_{\min} . In principle, with a higher degree of disorder, one might expect to have an increased number of trapping centers, all having the same energy gap. However, as shown in Fig. 4(a), the value of E_g is not constant, but increases systematically with disorder, i.e., E_g increases as T_{\min} increases. This observation is consistent with the picture of a growing fraction of localized carriers as disorder increases. Therefore, we conclude that the two-fluid model allows obtaining a simple and consistent picture of the temperature dependence of resistivity of SrRuO₃ and its dependence on disorder.

The two-fluid model has been proposed for metallic systems with strong electron-phonon coupling.¹⁸ Within this picture, E_g can be formally assimilated to the energy required for polaron formation and/or motion of dressed carriers. To what extent which SrRuO₃ belongs to a class of metals with

strong electron-phonon coupling is not definitely settled. Although through Raman scattering experiments it has been claimed that electron-phonon coupling is strong in SrRuO₃,²⁰ this remains an open issue, as the ferromagnetic transition is not affected by changing the oxygen isotope mass and the Jahn-Teller effect is negligible in SrRuO₃, indicating that electron-phonon coupling is weak.²¹ It should be noted that the model of Eq. (3) is *also* formally compatible with a picture in which carriers under the mobility edge undergo the Anderson localization. As the degree of disorder in the samples is varied, the mobility edge is shifted within the conduction band giving rise to a modulation of the number of localized electronic states. Thus, two different microscopic mechanisms might be formally represented by Eq. (3).

We note that in Eq. (3), we have assumed that the coefficient A_{ph} is related to electron-phonon scattering. Quite remarkably, we observe that the value of A_{ph} [extracted from fitting the experimental data to Eq. (3)] increases with disorder, as emphasized in Fig. 4(b) (open symbols), indicating that electron-phonon scattering is enhanced with disorder. If this conclusion is true, we should observe the same trend with disorder in the high-temperature region of $\rho(T)$, where the linear T dependence is related to the electron-phonon scattering. As discussed in the next section, we have observed indeed that the slope of $\rho(T)$ at temperatures above T_C is enhanced with disorder.

High-temperature region ($T > T_C$). We have observed that room temperature resistivity increases with disorder proportionally to the power-law index n extracted from fittings of low- T $\rho(T)$ to Eq. (1), and consequently, it increases proportionally also to T_{\min} . This is unambiguous evidence that effects of disorder on the high- T transport properties are correlated to those found at low temperature. A closer inspection of the data in the temperature range of $170 \text{ K} \leq T \leq 300 \text{ K}$ shows that the slope of $\rho(T)$ increases with disorder. The analysis of this linear high- T dependence has been performed within the usual electronic transport theory based on the electron-phonon coupling (Bloch-Grüneisen law), given by the expression²²

$$\rho = \rho_0 + \rho_m + \frac{2\pi k_B}{\hbar e^2 (n/m_{eff})} G(\Theta_D/T) \lambda' T = \rho_0 + \rho_m + \gamma(T) T, \quad (4)$$

where we have defined $\gamma(T) = [2\pi k_B] / [\hbar e^2 (n/m_{eff})] G(\Theta_D/T) \lambda'$. In Eq. (4), ρ_m is the magnetic resistivity due to spin scattering of electrons, which assumed to be constant above the ferromagnetic transition, n is the carrier density, m_{eff} the band effective mass, \hbar the Planck constant, e the electron charge, and $G(\Theta_D/T)$ is the Grüneisen function. As the dependence is clearly linear in the considered temperature interval, we can take $G(\Theta_D/T) \lambda' \equiv \lambda = \text{constant}$ and, thus, γ is also constant, where λ is the effective electron-phonon coupling constant, which is of the order of unity. Since the Debye temperature of SrRuO₃ has been estimated to be $\Theta_D \approx 368 \text{ K}$,³ the observed linear dependence appears at temperatures $T > 1/2\Theta_D$. The value of γ has been evaluated from the slope of the $\rho(T)$ curves in the temperature

range of $170 \text{ K} \leq T \leq 300 \text{ K}$, obtaining values of $0.6 \mu\Omega \text{ cm K}^{-1} \leq \gamma \leq 1.3 \mu\Omega \text{ cm K}^{-1}$ for different films. These values agree in order of magnitude with the value $\gamma \approx 0.5 \mu\Omega \text{ cm K}^{-1}$ calculated from Eq. (4) taking the experimentally determined values $n \approx 2 \times 10^{22} \text{ cm}^{-3}$ (Ref. 23), $m_{eff} \approx 3.7m_e$,³ and assuming that λ is of the order of the unity. Thus, the assumption of the validity of Eq. (4) appears to be reasonable, in spite of the reservations regarding the phononic origin of the high-temperature resistivity.²⁴ We observe that γ increases with T_{\min} [closed symbols in Fig. 4(b)], unequivocally indicating that the slope γ is enhanced as disorder increases.

Factors other than disorder, such as unintentional variation of film thickness, might, in principle, contribute to explain the systematic increase of residual resistivity and T_{\min} shown in Fig. 1 and, in turn, the tendencies displayed in Figs. 3 and 4. We argue, however, that disorder is the most essential factor. This observation is strongly supported by the effect of irradiation dose on the transport properties of the samples B1–B3. These specimens were prepared by cutting an original sample into three pieces (and, thus, B1–B3 have all the same thickness) and were subsequently irradiated with Ar⁺ ions accelerated at 100 keV at different doses up to 10^{13} ions/cm². At these ion energies and irradiation doses, the variation of thickness is entirely negligible.²⁵ Therefore, the increase of the slope of $\rho(T)$ in the high-temperature linear region with the irradiation dose displayed in Fig. 4(b) must necessarily be correlated to an increased disorder. This demonstrates that the observed behavior is neither due to any size effect nor to surface scattering contributions (Ref. 26) but driven by disorder.

This result is in manifest contradiction with reported theoretical calculations, which predict a systematic decrease of the slope as disorder increases,^{18,27} and is in contrast to the evolution with disorder of $\rho(T)$ observed in other complex electronic systems. An enhancement with disorder of the slope of the linear high-temperature dependence of $\rho(T)$ has also been observed in the Ce_{3-x}S₄ series (see Fig. 1 in Ref. 10). In that case, this phenomenon was attributed to the modulation of the number of itinerant carriers due to the depopulation of Ce 5d orbitals as the concentration of S increases.¹⁰ We believe that this is not our case, as the localization gaps range in the interval of $21 \text{ K} \leq E_g \leq 38 \text{ K}$ and, therefore, at room temperature, virtually all the electronic states should be delocalized, so that a depletion of free carriers is not probably the explanation of the increase of the electron-phonon scattering with disorder. Looking at Eq. (4), one might speculate about the increase of the electron-phonon coupling with disorder or about a systematic increase of the effective mass m_{eff} as disorder increases. Further work is needed to understand these effects.

In summary, we have made an extensive investigation of the temperature dependence of the resistivity $\rho(T)$ of SrRuO₃ thin films both at low and high temperatures. We have observed that the structural disorder modulates $\rho(T)$ in a systematic way. In the limit of low temperatures, we suggest that this modulation can be explained by assuming the presence of delocalized and/or localized electronic states, whose ratio is determined by the specific degree of disorder. In the high-temperature regime, the slope of the linear $\rho(T)$ in-

creases when disorder increases, in contrast to the reduction of slope with disorder observed in other strongly correlated electronic systems such as the A15 compounds. In the latter, the resistivity at high temperature rises more slowly than the linear dependence predicted by simple electron-phonon scattering theory, and indeed the resistivity tends to saturate as temperature increases. This resistivity saturation effect is more pronounced as disorder increases. However, these high-temperature anomalies are not observed in the $\rho(T)$ of SrRuO₃ for which $\rho(T)$ is linear, indicating a fundamental discrepancy with respect to other electronic complex materi-

als. Our observation reported here about the increase with disorder of the electron-phonon scattering contribution to the resistivity in SrRuO₃ films is an intriguing effect that should stimulate further theoretical and experimental works.

Financial support by the MEC of the Spanish Government (Projects NAN2004-9094-C03, MAT2005-5656-C04, and Nanoselect CSD2007-00041) and by the European Union [Project MaCoMuFi (FP6-03321) and FEDER] is acknowledged. G. H. acknowledges financial support from Generalitat de Catalunya (Spain).

*gherranz@icmab.es

- ¹C. B. Eom, R. J. Cava, R. M. Fleming, J. M. Phillips, R. B. van Dover, J. H. Marshall, J. W. P. Hsu, J. J. Krajewski, and W. F. Peck, *Science* **258**, 1766 (1992).
- ²L. Capogna *et al.*, *Phys. Rev. Lett.* **88**, 076602 (2002).
- ³P. B. Allen, H. Berger, O. Chauvet, L. Forro, T. Jarlborg, A. Junod, B. Revaz, and G. Santi, *Phys. Rev. B* **53**, 4393 (1996).
- ⁴Z. Fisk and G. W. Webb, *Phys. Rev. Lett.* **36**, 1084 (1976).
- ⁵M. Gurvitch, *Phys. Rev. B* **28**, 544 (1983).
- ⁶R. B. Laughlin, *Phys. Rev. B* **26**, 3479 (1982).
- ⁷M. Bibes, L. Balcells, S. Valencia, J. Fontcuberta, M. Wojcik, E. Jedryka, and S. Nadolski, *Phys. Rev. Lett.* **87**, 067210 (2001).
- ⁸M. Bibes, S. Valencia, L. Balcells, B. Martínez, J. Fontcuberta, M. Wojcik, S. Nadolski, and E. Jedryka, *Phys. Rev. B* **66**, 134416 (2002).
- ⁹E. Dagotto, T. Hotta, and A. Moreo, *Phys. Rep.* **344**, 1 (2001).
- ¹⁰M. Cutler, J. F. Leavy, and R. L. Fitzpatrick, *Phys. Rev.* **133**, A1143 (1964).
- ¹¹H. Lutz, H. Weismann, O. F. Kammerer, and M. Strongin, *Phys. Rev. Lett.* **36**, 1576 (1976).
- ¹²G. Herranz, F. Sánchez, J. Fontcuberta, M. V. García-Cuenca, C. Ferrater, M. Varela, T. Angelova, A. Cros, and A. Cantarero, *Phys. Rev. B* **71**, 174411 (2005).
- ¹³F. Sánchez, G. Herranz, I. C. Infante, J. Fontcuberta, M. V. García-Cuenca, C. Ferrater, and M. Varela, *Appl. Phys. Lett.* **85**, 1981 (2004).
- ¹⁴F. Sánchez, G. Herranz, J. Fontcuberta, M. V. García-Cuenca, C. Ferrater, and M. Varela, *Phys. Rev. B* **73**, 073401 (2006).
- ¹⁵I. Campbell and A. Fert, *Ferromagnetic Materials* (E. P. Wohlfarth, North-Holland, Amsterdam, 1982) Vol. 3.
- ¹⁶G. Herranz, B. Martínez, J. Fontcuberta, F. Sánchez, C. Ferrater, M. V. García-Cuenca, and M. Varela, *Phys. Rev. B* **67**, 174423 (2003).
- ¹⁷G. Herranz, F. Sánchez, J. Fontcuberta, V. Laukhin, J. Galibert, M. V. García-Cuenca, C. Ferrater, and M. Varela, *Phys. Rev. B* **72**, 014457 (2005).
- ¹⁸S. Kumar and P. Majumdar, *Phys. Rev. Lett.* **94**, 136601 (2005).
- ¹⁹L. R. Testardi, J. M. Poste, and H. J. Levinstein, *Phys. Rev. B* **15**, 2570 (1977).
- ²⁰M. N. Iliev, A. P. Litvinchuk, H.-G. Lee, C. L. Chen, M. L. Dezaneti, C. W. Chu, V. G. Ivanov, M. V. Abrashev, and V. N. Popov, *Phys. Rev. B* **59**, 364 (1999).
- ²¹G.-M. Zhao, K. Conder, H. Keller, and K. A. Müller, *Nature (London)* **381**, 676 (1996).
- ²²M. Gurvitch, A. K. Ghosh, B. L. Gyorffy, H. Lutz, O. F. Kammerer, J. S. Rosner, and M. Strongin, *Phys. Rev. Lett.* **41**, 1616 (1978).
- ²³L. Klein, J. S. Dodge, C. H. Ahn, G. J. Snyder, T. H. Geballe, M. R. Beasley, and A. Kapitulnik, *Phys. Rev. Lett.* **77**, 2774 (1996).
- ²⁴L. Klein, J. S. Dodge, C. H. Ahn, J. W. Reiner, L. Mieville, T. H. Geballe, M. R. Beasley, and A. Kapitulnik, *J. Phys.: Condens. Matter* **8**, 10111 (1996).
- ²⁵We have performed calculations of the sputtering yield for each of the atomic constituents of the target (SrRuO₃) using the the stopping and range of ions in matter (SRIM/TRIM) software package (www.srim.org). For Ar⁺ ions accelerated at 100 keV and assuming surface binding energies of Sr=1.7 eV, Ru=6.69 eV, and O=2 eV, we found from these calculations the following sputtering yields: ≈ 2 sputtered Sr atoms and/or ion; ≈ 0.6 sputtered Ru atoms and/or ion; ≈ 4 sputtered O atoms and/or ion. For a maximum irradiation dose of 10^{13} ions/cm², the total amount of sputtered material (adding up all the sputtered atoms) is, then, around 7×10^{13} ions/cm². Since the number of unit cells per surface is of the order of 5×10^{14} cm⁻², the total sputtered material corresponds to around 14% of a monolayer (i.e., the equivalent of an effective sputtered thickness of ~ 0.06 nm of SrRuO₃) for the film irradiated at the maximum dose.
- ²⁶J. W. C. de Vries, *Thin Solid Films* **167**, 25 (1988).
- ²⁷A. J. Millis, J. Hu, and S. Das Sarma, *Phys. Rev. Lett.* **82**, 2354 (1999).